

SMES: Towards Scalable Multi-Task Recommendation via Expert Sparsity

Yukun Zhang*, Si Dong*, Xu Wang*, Bo Chen, Qinglin Jia,

Shengzhe Wang, Jinlong Jiao, Runhan Li, Jiaqing Liu,

Chaoyi Ma[†], Ruiming Tang[†], Guorui Zhou, Han Li, Kun Gai

Kuaishou Technology Co., Ltd.

Beijing, China

{zhangyukun09,dongsi,wangxu28,renze03,dukang05,wangshengzhe,jiaojinlong,lirunhan}@kuaishou.com

{liujiqing,machaoyi03,tangruiming,zhouguorui,lihan08}@kuaishou.com,gai.kun@qq.com

Abstract

Industrial recommender systems typically rely on multi-task learning to estimate diverse user feedback signals and aggregate them for ranking. Recent advances in model scaling have shown promising gains in recommendation. However, naively increasing model capacity imposes prohibitive online inference costs and often yields diminishing returns for sparse tasks with skewed label distributions. This mismatch between uniform parameter scaling and heterogeneous task capacity demands poses a fundamental challenge for scalable multi-task recommendation. In this work, we investigate parameter sparsification as a principled scaling paradigm and identify two critical obstacles when applying sparse Mixture-of-Experts (MoE) to multi-task recommendation: **exploded expert** activation that undermines instance-level sparsity and **expert load skew** caused by independent task-wise routing. To address these challenges, we propose SMES, a scalable sparse MoE framework with **progressive expert routing**. SMES decomposes expert activation into a task-shared expert subset jointly selected across tasks and task-adaptive private experts, explicitly bounding per-instance expert execution while preserving task-specific capacity. In addition, SMES introduces a global **multi-gate load-balancing regularizer** that stabilizes training by regulating aggregated expert utilization across all tasks. SMES has been deployed in Kuaishou’s large-scale short-video services, supporting over 400 million daily active users. Extensive online experiments demonstrate stable improvements, with GAUC gain of **0.29%** and a **0.31%** uplift in user watch time.

CCS Concepts

• Information systems → Recommender systems; Personalization; • Computing methodologies → Multi-task learning.

Keywords

Multi-task Learning, Scalability, Recommender System

Permission to make digital or hard copies of all or part of this work for personal or classroom use is granted without fee provided that copies are not made or distributed for profit or commercial advantage and that copies bear this notice and the full citation on the first page. Copyrights for components of this work owned by others than the author(s) must be honored. Abstracting with credit is permitted. To copy otherwise, or republish, to post on servers or to redistribute to lists, requires prior specific permission and/or a fee. Request permissions from permissions@acm.org.

Conference acronym 'XX, Woodstock, NY

© 2018 Copyright held by the owner/author(s). Publication rights licensed to ACM.

ACM ISBN 978-1-4503-XXXX-X/2018/06

<https://doi.org/XXXXXXX.XXXXXXX>

ACM Reference Format:

Yukun Zhang, Si Dong, Xu Wang, Bo Chen, Qinglin Jia, Shengzhe Wang, Runhan Li, Jinlong Jiao, Jiaqing Liu, Chaoyi Ma, Ruiming Tang, Guorui Zhou, Han Li, Kun Gai. 2018. SMES: Towards Scalable Multi-Task Recommendation via Expert Sparsity. In *Proceedings of Make sure to enter the correct conference title from your rights confirmation email (Conference acronym 'XX)*. ACM, New York, NY, USA, 9 pages. <https://doi.org/XXXXXXX.XXXXXXX>

1 INTRODUCTION

Industrial recommender systems infer user preferences by modeling users’ historical interaction behaviors to deliver personalized recommendations, which have been widely deployed in platforms such as e-commerce, short-video services, and online advertising [12, 19, 34]. Owing to the lack of explicit user preference signals, practical recommender systems typically rely on multi-task learning frameworks [15, 17, 18, 21] to predict diverse dimensions of users’ implicit feedback. For example, in short-video recommendation scenarios like Kuaishou and TikTok [4, 23], recommender systems often simultaneously predict dozens or even hundreds of interaction probabilities, such as *Click, Like, Share, Comment, Long-view, and Completion*. To estimate users’ overall satisfaction with candidate items, these predictive probabilities are combined subsequently through aggregation functions or models [1, 2] to produce a final relevance or utility score for ranking.

Benefiting from advances in computational resources and the substantial gains brought by model scaling in the large language model (LLM) community [10, 25], many industrial recommender platforms have recently explored scaling approaches tailored to recommendation scenarios and achieved promising results (e.g., HSTU [27] and RankMixer [34]). However, industrial recommender systems operate under strict constraints of high concurrency and low latency, with stringent requirements on online inference [33]. Pursuing performance gains through parameter-scaling alone imposes significant burdens on online serving, ultimately harming system-level return on investment (ROI). Moreover, tasks across different data scale and sparsity regimes exhibit fundamentally distinct capacity demands [21, 23]. Figure 1 illustrates the performance trends of different tasks on the public KuaiRand dataset[9], as the model parameter scale increases. The results show that for some tasks (e.g., *like* and *follow*), scaling up model parameters does not lead to consistent performance improvements. The existing scaling methods [27, 34] often overlook the characteristics, and this misalignment between uniform capacity scaling and task-specific

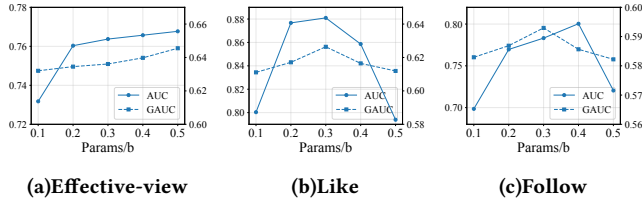


Figure 1: Performance trends across tasks in KuaiRand dataset. The curves show AUC (solid line) and GAUC (dashed line) trends with increasing model parameter scale (billion). For tasks (e.g., *watching-time task*, *Effective-view*), performance consistently improves with increasing parameter scale. In contrast, for tasks (e.g., *interaction tasks* such as *like* and *follow*), blindly increasing model capacity can lead to performance degradation.

supervision characteristics motivates adaptive scaling strategies for multi-task recommendation scenarios.

Therefore, we explore a new parameter scaling paradigm for multi-task recommendation, which simultaneously balances the performance gains from model scaling with stringent latency constraints and accommodates the heterogeneous capacity requirements of different tasks. Our core solution is parameter sparsification. On the one hand, sparse activation during online inference effectively alleviates latency overhead and reduces the computational cost induced by model scaling. On the other hand, sparsification enables different tasks to adaptively leverage an appropriate amount of model capacity, thereby avoiding unstable generalization caused by over-parameterization for sparse tasks.

Despite its appealing efficiency–capacity trade-off, directly applying sparse Mixture-of-Experts (MoE) to multi-task recommendation is non-trivial. Existing MoE systems typically balance experts per router or per task, which is sufficient in single-task settings but inadequate under multi-task sparse routing, where expert usage is aggregated across tasks at the instance level. MTL introduces multiple task-specific routers whose sparse decisions jointly determine the expert computation at inference time. In practice, naive task-wise sparse routing suffers from two fundamental issues. First, independent top- k routing across tasks leads to **exploded expert activation**. Different tasks may activate largely disjoint expert subsets for the same instance, causing the union of activated experts to grow rapidly with the number of tasks and undermining instance-level sparsity. Conversely, excessive overlap may collapse multiple tasks onto a small subset of experts, limiting effective capacity and task specialization. Second, sparse routing exacerbates **severe expert load skew** under MTL. Since expert updates are triggered only when selected, traffic and gradients from multiple tasks can accumulate on a few popular experts, while many others remain rarely activated and under-trained. Such imbalance becomes increasingly severe as the number of tasks grows, leading to unstable training dynamics and inefficient utilization of large expert pools.

To address these challenges, we propose SMES (Scalable Multi-task recommendation via Expert Sparsity), a sparse MoE framework that translates parameter scaling into consistent performance gains in multi-task recommendation. SMES introduces a **progressive expert routing mechanism** that decomposes expert activation into

an instance-level shared expert subset and a task-adaptive expert subset. By selecting a small set of shared experts jointly preferred by all tasks and allowing each task to activate a limited number of additional private experts, SMES explicitly controls exploded expert activation while preserving task-specific capacity. This design bounds the number of distinct experts executed per instance, enabling predictable and scalable inference under strict latency budgets. Furthermore, SMES employs a **multi-task load-balancing regularizer** that operates on aggregated expert usage across all tasks, rather than balancing each task router independently. This global regularization mitigates expert hotspots induced by multi-task sparse routing and stabilizes training as the expert pool scales. We also incorporate deployment-specific optimizations to enable efficient execution and maintain low-latency serving at scale.

Overall, the contributions are mainly summarized as follows:

- We identify and analyze the unique challenges of parameter scaling with sparse MoE in multi-task recommendation, highlighting the tension between scaling model capacity, task specialization, and aggregated expert utilization.
- We propose SMES, a sparse multi-gate MoE framework that enables efficient parameter scaling in multi-task recommendation via coordinated routing and cross-task load balancing.
- Extensive experiments on public benchmarks and large-scale industrial datasets demonstrate that SMES consistently outperforms classic dense and naive sparse baselines, achieving superior efficiency–capacity trade-offs under strict online serving constraints.
- We further develop an efficient online deployment and execution strategy for SMES, including optimized matrix computation and memory-efficient execution, supporting large-scale low-latency production serving on Kuaishou and yielding a 0.31% lift in user watch time.

2 RELATED WORK

This section briefly reviews the optimization research of multi-task learning (MTL) and model scaling in recommender systems.

2.1 Multi-Task Recommendation

For industrial recommendation, it is essential to predict multiple tasks simultaneously, such as Click, Like, Share, and other user interactions. Therefore, multi-task learning has been a key area of focus in industrial research for a long time.

Early methods relied on hard expert architectures such as shared bottom [3] and mixture-of-experts (MoE) [14], which were difficult to adapt to complex task relationships. Multi-gate Mixture-of-Experts (MMoE) [18] applied the MoE structure to multi-task learning and explicitly modeled task relationships through shared experts and task-specific gating, which performed better in low-relevance scenarios. To alleviate the seesaw phenomenon, progressive layer extraction (PLE) [21] separated shared and task-specific components and improved joint representation efficiency through progressive routing. Adaptive Task-to-Task Fusion Network (AdaTT) [16] further introduced residual and gating mechanisms to adaptively learn shared and task-specific knowledge via fusion units. Moreover, the Multi-Level Sparse Sharing Model

(MSSM) [6] designed field-level and unit-level sparse modules to address negative transfer caused by indistinguishable feature sharing. To tackle the parameter and resource bottlenecks of MoE-based methods, Mixture-of-Masked-Experts (MoME) [24] extracted experts from a base network using binary masks and reduced storage requirements through coarse and fine-grained pruning. Hierarchy of Multi-Gate Experts (HoME) [23] adopted expert normalization, hierarchical masking, and feature gating mechanisms to mitigate expert collapse, degradation, and underfitting.

2.2 Model Scaling

Due to the significant performance improvements brought by scaling up in the LLM field, recommendation models have also explored scaling strategies in recent years. Wukong [28] proposed a stacked factorization machine architecture and a collaborative scaling strategy, capturing arbitrary sequence feature interactions by increasing the number of layers and model width. HSTU [27] organized samples in a user-centric manner and designed a Hierarchical Sequential Transduction Unit to model sequential information, exploring the scaling of recommendation models through generative training approaches. HHFT [26] improved the model scaling scheme for large-scale heterogeneous feature scenarios through stacked heterogeneous Transformer and Hiformer [11] layers. Moreover, OneTrans [30] encoded sequential and non-sequential features into a unified token space and leveraged a shared Transformer block to jointly perform sequence modeling and feature interaction. Beyond the Transformer-based scaling strategies discussed above, RankMixer [34] explored a more efficient modeling paradigm by replacing self-attention with a multi-head token-mixing module combined with per-token feed-forward networks (FFNs) to enable efficient feature interaction, thereby scaling the model to one billion parameters. In addition, it adopted a sparse MoE architecture to improve overall ROI and alleviate expert training imbalance.

Despite the impressive results achieved by current model scaling approaches, they still face several challenges in industrial deployment. Industrial recommendation is constrained by high concurrency and low latency, and simply scaling parameters can easily increase service burden and reduce ROI. Furthermore, existing methods do not adapt to the heterogeneous capacity requirements of tasks with different sparsity, leading to suboptimal performance. Therefore, it is crucial to explore a new paradigm for scaling multi-task recommendation parameters that balances latency and performance while adapting to heterogeneous task capacities.

3 METHODOLOGY

3.1 Preliminaries

We consider a multi-task recommendation model trained on T prediction tasks $\mathcal{T} = \{1, \dots, T\}$ (e.g., click, effective-view, like). Each training instance is represented by an input feature vector $\mathbf{x} \in \mathbb{R}^d$ that concatenates user, item, and contextual features [5], paired with the associated labels $\mathbf{y} = \{y_t\}_{t=1}^T$.

Specifically, a shared encoder $F(\cdot)$ maps the input \mathbf{x} into a dense representation, capturing intrinsic user-item-context interactions. This encoder is typically instantiated as embedding layers followed by a deep representation learning backbone, such as DeepFM [13],

DCN [22], DIN [32], or SIM [19]:

$$\mathbf{h} = F(\mathbf{x}) \in \mathbb{R}^{d_{\text{in}}}. \quad (1)$$

Subsequently, a task-specific prediction head $\phi_t(\cdot)$ (e.g., Multi-Layer Perceptron) projects the shared representation \mathbf{h} to the prediction for task t :

$$\hat{y}_t = \phi_t(\mathbf{h}). \quad (2)$$

The overall training objective is a weighted sum of task losses:

$$\mathcal{L}_{\text{total}} = \sum_{t=1}^T \lambda_t \mathcal{L}_t(y_t, \hat{y}_t), \quad (3)$$

where $\lambda_t \geq 0$ serves as a hyper-parameter balancing the contribution of task t , and \mathcal{L}_t denotes the task-specific loss function (e.g., binary cross-entropy).

3.1.1 Dense Multi-Task MoE and Scaling Bottlenecks. A common baseline directly stacks task-specific heads on the shared representation, formulated as $\hat{y}_t = \phi_t(\mathbf{h})$. However, when tasks are heterogeneous (e.g., possessing distinct decision boundaries or generating partially conflicting gradients), forcing them to share the exact same feature subspace can restrict task specialization and induce negative transfer [29]. To facilitate *task-adaptive* feature sharing, MMoE [18] introduces a mixture-of-experts layer on top of \mathbf{h} . This architecture maintains a set of E experts $\{f_e\}_{e=1}^E$ and assigns a dedicated gate (router) g_t to each task t . Specifically, each expert $f_e : \mathbb{R}^{d_{\text{in}}} \rightarrow \mathbb{R}^{d_{\text{out}}}$ transforms the shared representation into an expert output \mathbf{o}_e , while each gate $g_t : \mathbb{R}^{d_{\text{in}}} \rightarrow \mathbb{R}^E$ generates routing logits \mathbf{z}_t over the experts. Concretely,

$$\begin{aligned} \mathbf{o}_e &= f_e(\mathbf{h}) \in \mathbb{R}^{d_{\text{out}}}, & e = 1, \dots, E, \\ \mathbf{z}_t &= g_t(\mathbf{h}) \in \mathbb{R}^E, \\ \mathbf{p}_t &= \text{softmax}(\mathbf{z}_t) \in \mathbb{R}^E, \\ \mathbf{h}_t &= \sum_{e=1}^E p_{t,e} \mathbf{o}_e \in \mathbb{R}^{d_{\text{out}}}, \end{aligned} \quad (4)$$

where \mathbf{p}_t lies on the probability simplex ($p_{t,e} \geq 0$ and $\sum_{e=1}^E p_{t,e} = 1$), and $p_{t,e}$ denotes the e -th entry of \mathbf{p}_t . The task-specific representation \mathbf{h}_t is then fed into the corresponding head: $\hat{y}_t = \phi_t(\mathbf{h}_t)$.

In principle, MoE capacity can be increased by scaling the number of experts E , thereby increasing parameters and allowing different experts to capture diverse patterns in recommendation data. However, most recommender deployments adopt **expert-dense** MoE variants, where all E experts are computed and then aggregated for each task. Consequently, both expert-side computation and intermediate activations scale linearly with E :

$$\text{FLOPs/instance} \propto E, \quad \text{ActMem/instance} \propto E, \quad (5)$$

which conflicts with strict online latency and memory budgets.

Moreover, tasks operating at varying data scales exhibit fundamentally distinct capacity demands [21, 23]. In industrial multi-task recommendation scenarios, tasks often encounter highly heterogeneous data regimes. While some tasks benefit from abundant supervision signals, others suffer from severe label sparsity and skewed distributions. This misalignment between static, dense model capacity and diverse task complexities inevitably leads to significant resource wastage and suboptimal serving efficiency.

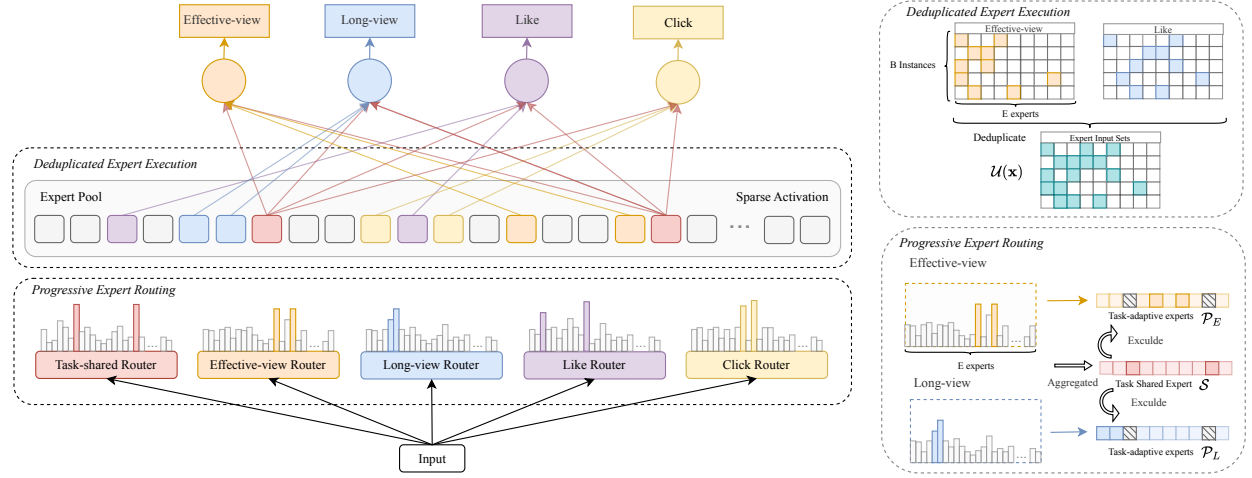


Figure 2: The architecture of our SMES for multi-task recommendation. It contains two key components: (1) Progressive Expert Routing uses a task-shared router and task-adaptive sub-routers to select experts (only Effective-view and Long-view tasks are visualized for clarity). (2) Deduplicated Expert Execution removes redundant expert computations across tasks.

3.1.2 Sparse MoE and MTL-Specific Challenges. To reconcile the conflict between capacity scaling and strict online latency budgets, and to adaptively match model capacity with diverse task complexities, we adopt *sparse routing*. This paradigm decouples the parameter size from the active computation per instance. In a standard single-task scenario, sparse MoE dynamically selects a subset of experts via a routing mechanism [8, 20]. Given router logits $\mathbf{z} \in \mathbb{R}^E$ over E experts, the set of activated indices is determined by:

$$\mathcal{K} = \text{TopK}(\mathbf{z}, K), \quad K \ll E, \quad (6)$$

where $\mathcal{K} \subset \{1, \dots, E\}$ denotes the index set of the K selected experts with the highest routing scores, and K denotes the routing budget. The *routing weights* are then computed by normalizing the probability mass strictly within the selected experts:

$$p_e = \frac{\exp(z_e)}{\sum_{j \in \mathcal{K}} \exp(z_j)} \cdot \mathbb{I}[e \in \mathcal{K}], \quad (7)$$

where $\mathbb{I}[\cdot]$ is the indicator function. The output is computed as $\tilde{\mathbf{h}} = \sum_{e \in \mathcal{K}} p_e \mathbf{o}_e$. Compared to dense MoE, sparse routing reduces the computational complexity from $O(E)$ to $O(K)$ per instance, theoretically enabling massive scaling of E .

Naive multi-task sparse routing. A straightforward extension to multi-task learning is to equip each task t with an independent router g_t and perform task-wise independent sparse routing. For an instance i_g , task t selects its top- K experts $\mathcal{K}_t = \text{TopK}(\mathbf{z}_t, K)$. However, in industrial recommendation where the number of tasks T is large, this naive design faces two critical challenges:

- **Exploded Expert Activation.** While each task respects the budget K , the system-level computational cost for processing instance i_g depends on the *union* of activated experts across all tasks, denoted as $\mathcal{U} = \bigcup_{t=1}^T \mathcal{K}_t$. The effective number of active

experts is bounded by:

$$K \leq |\mathcal{U}| \leq \min\{E, TK\}. \quad (8)$$

When tasks select disjoint sets of experts due to task diversity, $|\mathcal{U}|$ grows with T . Given that TK can easily exceed E in practice, this “union effect” causes the model to degenerate back into a dense-like regime (activating nearly all experts). By contrast, activating only K experts ($K \ll E$) can collapse tasks onto a small expert subset, limiting effective capacity.

- **Severe Expert Load Skew.** For a mini-batch of size B , the cumulative routing load for expert e is calculated by aggregating selections across all tasks and instances:

$$c_e = \sum_{b=1}^B \sum_{t=1}^T \mathbb{I}[e \in \mathcal{K}_t^{(b)}]. \quad (9)$$

As the load is aggregated across T independent routers, the resulting distribution $\{c_e\}_{e=1}^E$ tends to be severely skewed. This accumulation effect causes a small subset of experts to dominate traffic and gradients, while the majority remain underutilized and undertrained.

3.2 SMES: Scalable Multi-Task Recommendation via Expert Sparsity

To overcome the computational bottlenecks of dense MMoE (Sec. 3.1.1) while resolving the *exploded activation* and *load skew* pathologies inherent to naive multi-task sparse routing (Sec. 3.1.2), we propose **Scalable Multi-Task Recommendation via Expert Sparsity (SMES)**, as illustrated in Figure 2.

SMES retains the standard multi-task architecture (shared encoder F , expert pool $\{f_e\}_{e=1}^E$, and task heads $\{\phi_t\}_{t=1}^T$), while redesigning *expert routing and execution*. Specifically, SMES integrates two key components: **Progressive Expert Routing (PER)**, which strictly bounds the number of *distinct* experts executed

per instance to prevent activation explosion; and a **Multi-Task Load-Balancing (MTLB) Regularizer**, which mitigates cross-task hotspots to stabilize aggregated expert utilization.

3.2.1 Progressive Expert Routing

Task Routers. Following Eq. (4), each task router g_t maps the shared representation \mathbf{h} to logits $\mathbf{z}_t \in \mathbb{R}^E$. These logits are then normalized to obtain scores $\mathbf{p}_t = \text{softmax}(\mathbf{z}_t)$. Here, $z_{t,e}$ and $p_{t,e}$ denote the e -th entry of \mathbf{z}_t and \mathbf{p}_t , respectively.

We generalize the concept of shared and specific experts to a dynamic, sparse routing context. For each instance i_g per task, SMES activates only $K \ll E$ experts, decomposed as $K = K_s + K_a$, where K_s experts form a **task-shared** set across all tasks, and K_a experts are **task-adaptive** and selected separately for each task.

Stage-I: Task-shared experts. We compute a **global routing score** for each expert by weighted pooling *normalized* task-specific routing probabilities:

$$s_e = \sum_{t=1}^T w_t p_{t,e}, \quad (10)$$

where $w_t \geq 0$ is an optional task weight that reflects task importance (default $w_t = 1$). The shared expert set is then selected as

$$\mathcal{S} = \text{TopK}(\{s_e\}_{e=1}^E, K_s), \quad |\mathcal{S}| = K_s. \quad (11)$$

Stage-II: Task-adaptive experts. For each task t , we select K_a additional experts from the remaining candidates (complement of \mathcal{S}) based on the corresponding logits $z_{t,e}$:

$$\mathcal{A}_t = \text{TopK}(\{z_{t,e}\}_{e \notin \mathcal{S}}, K_a), \quad |\mathcal{A}_t| = K_a. \quad (12)$$

The final activated set for task t is:

$$\mathcal{K}_t = \mathcal{S} \cup \mathcal{A}_t, \quad |\mathcal{K}_t| = K. \quad (13)$$

By construction, all tasks share \mathcal{S} , guaranteeing a minimum overlap of K_s experts per instance, while \mathcal{A}_t preserves task-adaptive capacity.

Deduplicated Expert Execution. Given the activated sets $\{\mathcal{K}_t\}_{t=1}^T$, a naive sparse implementation executes experts independently for each task, redundantly recomputing \mathbf{o}_e whenever multiple tasks activate the same expert. SMES removes this redundancy by executing each selected expert *at most once per instance* on the cross-task set:

$$\mathcal{U} = \bigcup_{t=1}^T \mathcal{K}_t, \quad |\mathcal{U}| \leq K_s + T K_a. \quad (14)$$

We then compute expert outputs \mathbf{o}_e only for the experts $e \in \mathcal{U}$. The resulting outputs $\{\mathbf{o}_e\}_{e \in \mathcal{U}}$ are shared across all tasks in the subsequent aggregation, reducing expert executions per instance from up to TK to $|\mathcal{U}|$.

Sparse Aggregation. Given \mathcal{K}_t and the computed expert outputs, we compute the final routing weights $p_{t,e}$ by renormalizing *only* over activated experts:

$$p_{t,e} = \frac{\exp(z_{t,e})}{\sum_{j \in \mathcal{K}_t} \exp(z_{t,j})} \cdot \mathbb{I}[e \in \mathcal{K}_t]. \quad (15)$$

The task-specific representation is $\mathbf{h}_t = \sum_{e \in \mathcal{K}_t} p_{t,e} \mathbf{o}_e$, followed by the task head $\hat{y}_t = \phi_t(\mathbf{h}_t)$.

3.2.2 Multi-Task Load-Balancing Regularization. To prevent *cross-task* expert hotspots under multi-task top- K routing, we regularize expert utilization by balancing the *aggregate* traffic induced by *all* task routers. For a mini-batch of size B , we define the *selection frequency* \bar{f}_e and the *probability mass* \bar{p}_e for expert e as

$$\begin{aligned} \bar{f}_e &= \frac{1}{BT} \sum_{b=1}^B \sum_{t=1}^T \mathbb{I}[e \in \mathcal{K}_t^{(b)}], \\ \bar{p}_e &= \frac{1}{BT} \sum_{b=1}^B \sum_{t=1}^T p_{t,e}^{(b)}. \end{aligned} \quad (16)$$

where $\mathcal{K}_t^{(b)}$ denotes the experts activated by task t for the b -th instance in the mini-batch. We then minimize

$$\mathcal{L}_{\text{lb}} = \frac{E}{K} \sum_{e=1}^E \bar{f}_e \bar{p}_e, \quad (17)$$

which discourages concentrating *both* high realized traffic (\bar{f}_e) and high routing preference (\bar{p}_e) on the same experts *across tasks*. This couples the T routers and directly targets system-level imbalance where a few experts become overloaded jointly by multiple tasks.

The overall training objective is

$$\mathcal{L} = \mathcal{L}_{\text{task}} + \beta \mathcal{L}_{\text{lb}}, \quad (18)$$

where $\beta \geq 0$ controls the regularization strength.

3.3 Deployment and System Optimizations

The sparse multi-task design introduces two practical challenges for online deployment. First, deduplicated routing leads to varying input shapes across batches, resulting in irregular execution patterns that limit the applicability of static compilation and kernel-level optimizations. Second, such dynamic execution necessitates per-batch memory allocation. These factors introduce additional runtime overhead and hinder the effective utilization of computational resources. We address these challenges via a custom deduplicated expert kernel and profiling-guided workspace allocator.

3.3.1 Reindexed Grouped GEMM. The construction of the deduplicated expert set \mathcal{U} inherently produces *ragged tensors*, where each expert processes a varying, non-contiguous subset of the mini-batch. Standard dense matrix multiplications cannot efficiently support such irregular patterns. To resolve this, we propose a **Reindexed Grouped GEMM** kernel. Inspired by MegaBlocks [7], this design maps dynamic sparse activations directly into compact dense computations, bypassing variable-shape overheads. The pipeline proceeds in four phases:

Traffic Calculation. For a mini-batch of size B , let $b \in \{1, \dots, B\}$ index the instances and $e \in \{1, \dots, E\}$ index the experts. $\mathcal{U}^{(b)}$ denotes the set of unique experts required by instance b across all tasks. We define the effective load for expert e as $n_e = \sum_{b=1}^B \mathbb{I}[e \in \mathcal{U}^{(b)}]$. The total number of active expert executions is $N_{\text{act}} = \sum_{e=1}^E n_e$.

Execution-Time Reindexing (Gather & Map). Standard frameworks struggle with dynamic tensor shapes. We explicitly manage memory by gathering inputs into a static workspace.

- **Gather:** We gather hidden states \mathbf{x} of instances activating expert e into a compact matrix. All such matrices are packed contiguously into a global tensor $\mathbf{X} \in \mathbb{R}^{N_{\text{act}} \times d_{\text{in}}}$.
- **Index Mapping (π):** Simultaneously, we record a back-mapping π . For every activated pair (b, e) , $\pi(b, e)$ stores the row index in \mathbf{X} corresponding to this computation.

Grouped GEMM. We perform expert computations in a single batched kernel:

$$\mathbf{O} = \text{GroupedGEMM}(\mathbf{X}, \{\mathbf{W}_e\}, \{n_e\}), \quad (19)$$

where each expert weight \mathbf{W}_e is applied to its corresponding contiguous segment of \mathbf{X} with size n_e , and $\mathbf{O} \in \mathbb{R}^{N_{\text{act}} \times d_{\text{out}}}$ stores the resulting expert outputs.

Task-wise Representation Reconstruction. Finally, we recover task-specific representations $\mathbf{h}_t^{(b)}$ by querying the packed results using the map π :

$$\mathbf{h}_t^{(b)} = \sum_{e \in \mathcal{K}_t^{(b)}} p_{t,e}^{(b)} \cdot \mathbf{O}[\pi(b, e)]. \quad (20)$$

This ensures that if multiple tasks select the same expert for an instance, the expert is evaluated exactly once, and the result is reused via the index map.

3.3.2 Profiling-Guided Workspace Allocation. Due to deduplicated sparse routing, the number of expert executions N_{act} varies significantly across batches, leading to fluctuating workspace requirements. Consequently, the temporary workspace required M_{req} for the packed inputs \mathbf{X} and expert outputs \mathbf{O} varies linearly:

$$M_{\text{req}} \propto N_{\text{act}} \cdot (d_{\text{in}} + d_{\text{out}}). \quad (21)$$

To balance memory efficiency and latency, we implement a profiling-guided workspace allocation strategy. Based on offline profiling of the load distribution $P(N_{\text{act}})$, we pre-allocate a shared GPU memory pool composed of a set of fixed-size memory pages, where each page roughly corresponds to the memory footprint required for processing a single item. At runtime, after determining the required number of active pages, each execution thread allocates a contiguous block of pages from the shared pool and releases them back to the pool upon completion of expert computation. By leveraging offline profiling to estimate the expected concurrency level, we provision the pool capacity to reduce contention-induced waiting while maximizing overall memory utilization.

3.4 Discussion

We discuss the computational complexity and scalability of SMES against the standard dense MMoE variant.

- **Dense MMoE:** In standard MMoE, every instance is processed by all E experts. Consequently, both FLOPs and memory costs scale linearly with the number of experts $O(E)$, making large-scale deployment increasingly expensive.
- **SMES:** SMES decouples inference cost from the total model capacity. With sparse routing and deduplicated execution (Sec. 3.2.1), inference only evaluates the set of unique activated experts \mathcal{U} , resulting in a computational complexity of $O(|\mathcal{U}|)$. Since $|\mathcal{U}| \ll E$ due to the task-shared expert set \mathcal{S} , the inference cost is significantly lower than $O(E)$, ensuring both sparsity and scalability as

Table 1: Dataset of public KuaiRand and industrial Kuaishou

Dataset	Users	Items	Instances	Features	#Tasks
KuaiRand-1K	1,000	4,369,953	1.17×10^7	92	12
Kuaishou	4×10^9	3×10^8	5×10^{10}	326	21

the number of experts expands. Meanwhile, the proposed multi-task load-balancing regularization (Sec. 3.2.2) promotes balanced expert utilization under sparse activation, maintaining training stability. Finally, our online optimization strategies (Sec. 3.3) further ensure that the sparse design translates into bounded and stable serving latency in real-world deployments.

4 Experiments

4.1 Experiment Settings

4.1.1 Datasets. We adopt KuaiRand-1K a benchmark recommendation dataset (detailed in Table 1), as the public dataset for offline experiments, and simultaneously conduct large-scale industrial offline studies on the Kuaishou short-video recommendation platform. To maintain consistent terminology, the valid_play label in KuaiRand-1K is mapped to Effective-view. The industrial dataset comprises 400 million users and generates 50 billion daily interaction logs. Each sample corresponds to a user-video pair and the associated feedback, representing a recommendation interaction. To align with practical industrial requirements, we focus on four key prediction tasks: **Effective-view**, **Long-view**, **Click**, and **Like**.

4.1.2 Baselines. We compare SMES with representative multi-task learning methods: **MMoE**, the standard multi-expert framework for recommendation; **PLE**, which alleviates the seesaw phenomenon by separating shared and task-specific components; **MoME**, which applies parameter sparsification to balance performance and resource usage; and **HoME**, a MoE-based framework successfully deployed in large-scale industrial recommendation systems using hierarchical masking for stability. We also evaluate **RankMixer**, which leverages sparse MoE for parameter scaling.

4.1.3 Evaluation Metrics. We evaluate our model using two widely adopted ranking metrics: **AUC** and **GAUC**, with GAUC being the primary offline metric in our short-video recommendation service [31]. GAUC computes the AUC independently for each user and aggregates them in a weighted manner:

$$\text{GAUC} = \sum_u w_u \cdot \text{AUC}_u, \quad \text{where} \quad w_u = \frac{\#\text{samples}_u}{\sum_i \#\text{samples}_i}$$

where w_u denotes the user's sample proportion.

4.2 Offline Experiments

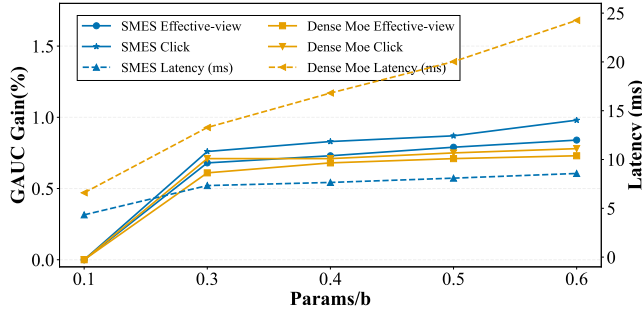
This section validates the effectiveness and generalization of SMES on recommendation tasks. Table 2 presents the offline evaluation results on two real-world datasets: KuaiRand-1K and Kuaishou, with models grouped by similar parameter budgets.

As shown in Table 2, PLE consistently outperforms MMoE on most tasks, indicating that explicitly separating shared and task-specific components is beneficial for mitigating inter-task interference. In contrast, MoME shows relatively weaker performance

Table 2: Offline results on public KuaiRand-1K and Kuaishou industrial datasets. Boldface denotes the highest score and underline indicates the best result of the baselines.

Model	KuaiRand-1K Dataset										Kuaishou Industrial Dataset									
	Effective-view		Like		Follow		Comment		#Params	Effective-view		Long-view		Click		Like		#Params		
	AUC	GAUC	AUC	GAUC	AUC	GAUC	AUC	GAUC		AUC	GAUC	AUC	GAUC	AUC	GAUC	AUC	GAUC			
MMoE	0.7657	0.6355	0.8586	0.6119	0.8004	0.6188	0.7855	0.5957	386.84M	0.7867	0.7319	0.8223	0.7645	0.7370	0.6663	0.9650	0.8479	243.96M		
PLE	0.7670	0.6363	<u>0.8939</u>	<u>0.6280</u>	0.7989	<u>0.6220</u>	0.8274	0.5990	387.79M	0.7875	0.7325	0.8220	0.7640	0.7363	0.6659	0.9647	0.8476	251.16M		
HoME	0.7672	0.6417	0.8891	0.6251	0.7973	0.5997	0.7994	<u>0.6031</u>	387.31M	0.7876	0.7332	0.8204	0.7626	0.7322	0.6664	0.9650	0.8477	269.66M		
MoME	0.7667	0.6313	0.8384	0.6201	0.8033	0.5922	0.7988	0.5943	389.68M	0.7866	0.7319	0.8220	0.7641	0.7367	0.6660	0.9649	0.8478	271.47M		
Rankmixer	0.7699	<u>0.6419</u>	0.8818	0.6230	<u>0.8060</u>	0.5975	<u>0.8301</u>	0.5932	387.31M	0.7890	<u>0.7342</u>	0.8234	0.7658	0.7295	0.6665	<u>0.9651</u>	<u>0.8488</u>	280.90M		
SMES-S	0.7722	0.6426	0.9102	0.6284	0.8075	0.6224	0.8465	0.6046	386.13M	0.7895	0.7356	0.8235	0.7663	0.7419	0.6690	0.9655	0.8492	272.70M		
Improved	+0.23%	+0.07%	+1.63%	+0.04%	+0.15%	+0.04%	+1.64%	+0.15%	-	+0.05%	+0.14%	+0.01%	+0.05%	+0.49%	+0.25%	+0.04%	+0.04%	-		
SMES-L	0.7741	0.6448	0.9182	0.6309	0.8159	0.6251	0.8502	0.6052	510M	0.7918	0.7371	0.8241	0.7671	0.7424	0.6712	0.9663	0.8499	633M		
Improved	+0.42%	+0.22%	+2.43%	+0.29%	+0.99%	+0.31%	+2.01%	+0.21%	-	+0.28%	+0.29%	+0.07%	+0.13%	+0.54%	+0.47%	+0.12%	+0.11%	-		

SMES-S and SMES-L denote two scaled configurations of SMES. SMES-S matches the parameter budget of the baselines, whereas SMES-L increases expert capacity under a fixed sparsity ratio of 8% to explore the performance ceiling.

**Figure 3: Scalability Analysis of SMES vs. Dense MoE: Performance and Latency in Effective View and Click Tasks.**

across tasks, suggesting that naive parameter sparsification may compromise representation capacity. RankMixer, which emphasizes scalable sparse modeling, achieves competitive results and outperforms most baselines. SMES-S, a configuration of SMES designed to match the parameter budgets of representative baselines, delivers superior performance across all tasks on both public and industrial datasets. In particular, when compared to RankMixer, SMES-S obtains an average GAUC gain of around 0.1% on watching-time tasks (e.g., Effective-view), while delivering substantial gains on interaction tasks (e.g., Click, Like). These results highlight that SMES effectively addresses the misalignment between uniform capacity scaling and task-specific supervision. To further investigate the scalability of SMES, we scale up the model’s parameters while maintaining a comparable number of activated parameters to the baselines (i.e., variant SMES-L with expert sparsity of 8%). As shown in the results, SMES-L brings further improvements over SMES-S on all tasks, demonstrating that SMES can effectively leverage additional model capacity to improve performance. Together with the analysis in Section 4.3, these findings indicate that SMES yields significant gains without incurring additional latency overhead.

4.3 Scalability Analysis

This section presents the scaling curves for SMES and dense models with respect to parameter size, systematically evaluating scalability, task-adaptive capacity allocation, and latency efficiency. As

Table 3: Ablation Study of SMES Components with GAUC.

Dataset	Task	ours	w/o Task-SHA	w/o Task-ADA	w/o Reg
KuaiRand-1K	Effective-view	0.6426	0.6342	0.6409	0.6422
	Like	0.6284	0.6017	0.6010	0.6135
	Follow	0.6224	0.6198	0.6144	0.6174
	Comment	0.6046	0.5891	0.6045	0.5956
Kuaishou	Effective-view	0.7356	0.7344	0.7342	0.7345
	Long-view	0.7663	0.7650	0.7648	0.7649
	Click	0.6690	0.6670	0.6666	0.6681
	Like	0.8492	0.8484	0.8481	0.8483

shown in Figure 3, SMES consistently benefits from parameter scaling across heterogeneous tasks, effectively overcoming the diminishing returns observed in dense models. Its sparse structure and dynamic expert activation mechanism enable task-adaptive capacity allocation, providing superior performance relative to the dense baseline. In contrast, SMES maintains stable inference latency even as model parameters increase, satisfying the strict online serving constraints of industrial recommender systems. For instance, expanding SMES to 0.6B parameters results in an average GAUC improvement of 0.84% while incurring only a 4ms latency increase. However, dense models exhibit nearly linear latency growth with scale, limiting their practical deployment. These results validate that SMES balances parameter scaling, task specialization, and latency, establishing a practical paradigm for multi-task recommendation.

4.4 Ablation Study

We conduct ablation experiments on the public KuaiRand-1K and the Kuaishou industrial datasets to validate the effectiveness of three core SMES components, namely Task-shared experts (**w/o** Task-SHA), Task-adaptive experts (**w/o** Task-ADA), and load balancing regularization (**w/o** Reg). The full SMES model attains better GAUC performance than all ablation variants across all tasks on both datasets, which verifies the synergistic effect of its core components. Removing Task-SHA leads to significant performance degradation. This aligns with our method, which prioritizes the selection of shared experts from the expert pool to capture cross-task patterns. Removing Task-ADA also causes notable performance drops, highlighting the necessity of task-adaptive capacity allocation for

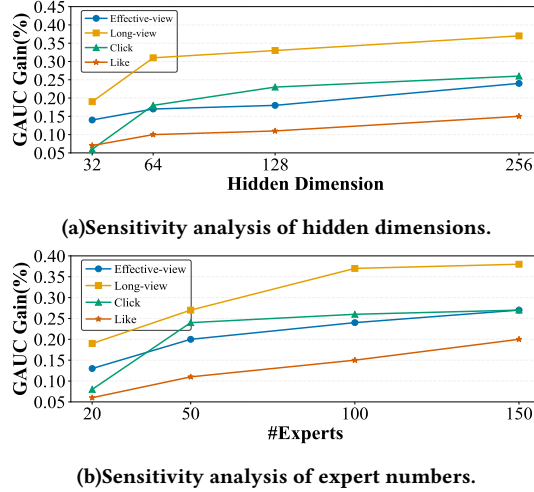


Figure 4: Hyper-Parameter Sensitivity of SMES. We evaluate the impact of hidden dimensions and expert numbers on SMES performance across core recommendation tasks (Effective-view, Like, Follow, Comment).

intra-task specialization. Removing load-balancing regularization leads to a moderate performance drop. This indicates that the regularizer plays an important role in mitigating expert overload by coordinating the aggregated activation across all tasks.

4.5 Hyper-Parameter Sensitivity

We examine the hyperparameter sensitivity of SMES with respect to the hidden dimension size and the number of experts to evaluate the model’s robustness and scalability. For the hidden dimension analysis, we fix the number of experts at 100 and evaluate four distinct dimension settings. For the expert count analysis, we fix the hidden dimension at 256 and assess four different settings for the number of experts. Experimental results in Figure 4a reveal a positive correlation between hidden dimension and model performance: the prediction accuracy exhibits a steady upward trend as the hidden dimension expands, while core metrics also demonstrate continuous and statistically meaningful improvements. From Figure 4b, it can be observed that model performance exhibits an overall upward trend with increasing expert count, where the GAUC continuously improves and reaches its optimal value at the maximum expert count. Hidden dimension expansion delivers relatively modest improvements overall, whereas increasing the number of experts brings more pronounced performance gains by comparison. Furthermore, different tasks exhibit varying sensitivities to parameter adjustments, with the Long-view task showing the strongest response to such changes across all tasks.

4.6 Visualization of Task-Expert Activation

To verify the effectiveness of adaptive expert selection across distinct tasks, we select the three most-activated and three least-activated tasks and extract the experts they activate, as shown in Figure 5. It can be observed that the number of activated experts for each task is adaptively matched to its data scale: dense tasks activate more experts for superior preference modeling, while sparse

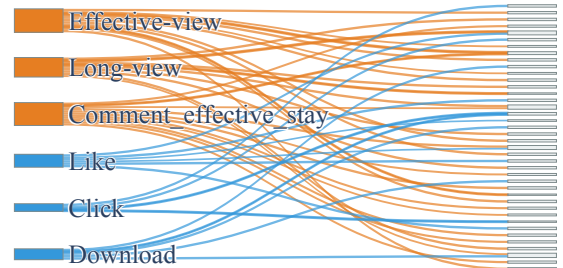


Figure 5: Task-Expert Activation of our SMES. For the sake of clarity and conciseness, we only display three most-activated with a high number of assigned experts, marked in orange, and three least-activated tasks with a low number, marked in blue.

tasks use fewer experts to prevent over-parameterization. Meanwhile, the balanced activation distribution across all tasks vividly demonstrates the exceptional effectiveness of the load-balancing regularization in SMES, which guarantees efficient and balanced expert utilization to underpin the scalable performance.

4.7 Online A/B Test

To evaluate the industrial feasibility of SMES, we conducted online A/B tests on the Kuaishou Single Page with 3.5% of production traffic from October 25 to October 31, 2025. To ensure the fairness of the A/B test, we only replaced HoME [23] in the baseline with the SMES module while keeping other components and hyperparameters unchanged. Online A/B test results validate that SMES achieves statistically significant improvements across all business-critical metrics, outperforming the baseline by a substantial margin. In the Kuaishou Single Page scenario, SMES delivers an average user watch time lift of +0.31%. Core interaction metrics also obtain notable and statistically meaningful gains, including Like +0.64%, Follow +1.56%, Comment +2.45%. SMES mitigates the trade-off between parameter scaling and inference latency, reducing inference latency by 50% relative to the dense MoE baseline with comparable capacity. SMES has been fully deployed in Kuaishou’s large-scale production environment, serving over 400 million users daily.

5 Conclusion

We present SMES, a scalable sparse MoE framework for multi-task recommendation that addresses the misalignment between uniform parameter scaling and heterogeneous task capacities. SMES uses progressive expert routing, splitting activation into a task-shared subset for universal patterns and task-adaptive experts for specialized modeling, thereby bounding the number of active experts per instance. A global load-balancing regularizer mitigates cross-task expert overload, and optimized matrix computation with efficient memory allocation enables low-latency deployment. Extensive experiments on public benchmarks and large-scale industrial datasets demonstrate that SMES consistently surpasses dense and naive sparse MoE baselines, achieving substantial online gains under strict latency budgets.

References

- [1] Jiangxia Cao et al. 2025. Pantheon: Personalized Multi-Objective Ensemble Sort via Iterative Pareto Policy Optimization. In *Proceedings of the 34th ACM International Conference on Information and Knowledge Management (CIKM)*. 5575–5582.
- [2] Yang Cao, Changhao Zhang, Xiaoshuang Chen, Kaiqiao Zhan, and Ben Wang. 2025. xMTF: A Formula-Free Model for Reinforcement-Learning-Based Multi-Task Fusion in Recommender Systems. In *Proceedings of the ACM on Web Conference (WWW)*. 3840–3849.
- [3] Rich Caruana. 1997. Multitask Learning. In *Machine Learning*, Vol. 28. 41–75.
- [4] Zheng Chai et al. 2025. Longer: Scaling Up Long Sequence Modeling in Industrial Recommenders. In *Proceedings of the 19th ACM Conference on Recommender Systems (RecSys)*. 247–256.
- [5] Bo Chen, Yichao Wang, Zhirong Liu, Ruiming Tang, Wei Guo, Hongkun Zheng, Weiwei Yao, Muyu Zhang, and Xiuqiang He. 2021. Enhancing explicit and implicit feature interactions via information sharing for parallel deep CTR models. In *Proceedings of the 30th ACM international conference on information & knowledge management*. 3757–3766.
- [6] Ke Ding et al. 2021. MSSM: A Multiple-level Sparse Sharing Model for Efficient Multi-Task Learning. In *Proceedings of the 44th International ACM SIGIR Conference on Research and Development in Information Retrieval*.
- [7] Trevor Droppo et al. 2022. MegaBlocks: Efficient Sparse Training with Mixture-of-Experts. In *MLSys*.
- [8] William Fedus, Barret Zoph, and Noam Shazeer. 2022. Switch Transformers: Scaling to Trillion Parameter Models with Simple and Efficient Sparsity. *Journal of Machine Learning Research* 23, 120 (2022), 1–39.
- [9] Chongming Gao, Shijun Li, Yuan Zhang, Jiawei Chen, Biao Li, Wenqiang Lei, Peng Jiang, and Xiangnan He. 2022. Kuairand: An unbiased sequential recommendation dataset with randomly exposed videos. In *Proceedings of the 31st ACM international conference on information & knowledge management*. 3953–3957.
- [10] Aaron Grattafiori et al. 2024. The Llama 3 Herd of Models. *arXiv preprint arXiv:2407.21783* (2024).
- [11] Huan Gui, Ruoxi Wang, Ke Yin, Long Jin, Maciej Kula, Taibai Xu, Lichan Hong, and Ed H. Chi. 2023. Hiformer: Heterogeneous Feature Interactions Learning with Transformers for Recommender Systems. *arXiv preprint arXiv:2311.05884* (2023).
- [12] Hufeng Guo, Bo Chen, Ruiming Tang, Weinan Zhang, Zhenguo Li, and Xiuqiang He. 2021. An Embedding Learning Framework for Numerical Features in CTR Prediction. In *Proceedings of the 27th ACM SIGKDD Conference on Knowledge Discovery & Data Mining (KDD)*. 2910–2918.
- [13] Hufeng Guo, Ruiming Tang, Yuming Ye, Zhenguo Li, and Xiuqiang He. 2017. DeepFM: A Factorization-Machine based Neural Network for CTR Prediction. In *Proceedings of the 26th International Joint Conference on Artificial Intelligence (IJCAI)*. 1725–1731.
- [14] Robert A. Jacobs, Michael I. Jordan, Steven J. Nowlan, and Geoffrey E. Hinton. 1991. Adaptive Mixtures of Local Experts. In *Neural Computation*, Vol. 3. 79–87.
- [15] Qinglin Jia, Zhaocheng Du, Chuhuan Wu, Hufeng Guo, Ruiming Tang, Shuting Shi, and Muyu Zhang. 2025. No One Left Behind: How to Exploit the Incomplete and Skewed Multi-Label Data for Conversion Rate Prediction. *arXiv preprint arXiv:2512.13300* (2025).
- [16] Danwei Li et al. 2023. AdaTT: Adaptive Task-to-Task Fusion Network for Multi-task Learning in Recommendations. In *arXiv*. *arXiv preprint arXiv:2304.04959*.
- [17] Xiaofan Liu, Qinglin Jia, Chuhuan Wu, Jingjie Li, Dai Quanyu, Lin Bo, Rui Zhang, and Ruiming Tang. 2023. Task adaptive multi-learner network for joint CTR and CVR estimation. In *Companion Proceedings of the ACM Web Conference 2023*. 490–494.
- [18] Jiaqi Ma, Zhe Zhao, Xinyang Yi, Jilin Chen, Lichan Hong, and Ed H. Chi. 2018. Modeling Task Relationships in Multi-task Learning with Multi-gate Mixture-of-Experts. In *Proceedings of the 24th ACM SIGKDD International Conference on Knowledge Discovery & Data Mining (KDD)*. 1930–1939.
- [19] Qi Pi, Weijie Zhou, Yingtong Zhang, Zhibin Liu, Rangkai Wang, Ying Ren, Guoqiang Fan, Xueyi Xiao, and Xiaoqiang Zhu. 2020. Search-based User Interest Modeling with Lifelong Sequential Behavior Data for Click-Through Rate Prediction. In *Proceedings of the 29th ACM International Conference on Information & Knowledge Management (CIKM)*. 2685–2692.
- [20] Noam Shazeer, Azalia Mirhoseini, Krzysztof Maziarz, Andy Davis, Quoc Le, Geoffrey Hinton, and Jeff Dean. 2017. Outrageously Large Neural Networks: The Sparsely-Gated Mixture-of-Experts Layer. In *Proceedings of the International Conference on Learning Representations (ICLR)*.
- [21] Hongyan Tang, Junning Liu, Ming Zhao, and Xudong Gong. 2020. Progressive Layered Extraction (PLE): A Novel Multi-Task Learning (MTL) Model for Personalized Recommendations. In *Proceedings of the 14th ACM Conference on Recommender Systems (RecSys)*. 269–278.
- [22] Ruoxi Wang, Bin Fu, Gang Fu, and Mingliang Wang. 2017. Deep & Cross Network for Ad Click Predictions. In *Proceedings of the AdKDD & TargetAd Workshop*. 1–7.
- [23] Xu Wang, Jiangxia Cao, Zhiyi Fu, Kun Gai, and Guorui Zhou. 2025. HOME: Hierarchy of Multi-Gate Experts for Multi-Task Learning at Kuaishou. In *Proceedings of the 31st ACM SIGKDD Conference on Knowledge Discovery and Data Mining (KDD)*. 2638–2647.
- [24] Jiahui Xu, Lu Sun, and Dengji Zhao. 2024. MoME: Mixture-of-Masked-Experts for Efficient Multi-Task Recommendation. In *Proceedings of the 47th International ACM SIGIR Conference on Research and Development in Information Retrieval*.
- [25] An Yang et al. 2025. Qwen3 Technical Report. *arXiv preprint arXiv:2505.09388* (2025).
- [26] Liren Yu, Wenming Zhang, Silu Zhou, Zhixuan Zhang, and Dan Ou. 2025. HHFT: Hierarchical Heterogeneous Feature Transformer for Recommendation Systems. In *Proceedings of the ACM Web Conference*.
- [27] Jiaqi Zhai et al. 2024. Actions Speak Louder than Words: Trillion-Parameter Sequential Transducers for Generative Recommendations. *arXiv preprint arXiv:2402.17152* (2024).
- [28] Buyun Zhang et al. 2024. Wukong: Towards a Scaling Law for Large-Scale Recommendation. In *Proceedings of the 41st International Conference on Machine Learning (ICML)*. 59421–59434.
- [29] Yu Zhang and Qiang Yang. 2021. A survey on multi-task learning. *IEEE transactions on knowledge and data engineering* 34, 12 (2021), 5586–5609.
- [30] Zhaoqi Zhang, Haolei Pei, Jun Guo, Tianyu Wang, Yufei Feng, Hui Sun, Shaowei Liu, and Aixin Sun. 2025. OneTrans: Unified Feature Interaction and Sequence Modeling with One Transformer in Industrial Recommender. *arXiv preprint arXiv:2510.26104* (2025).
- [31] Guorui Zhou, Xiaoqiang Zhu, Chenru Song, Ying Fan, Han Zhu, Xiao Ma, Yanghui Yan, Junqi Jin, Han Li, and Kun Gai. 2018. Deep interest network for click-through rate prediction. In *Proceedings of the 24th ACM SIGKDD international conference on knowledge discovery & data mining*. 1059–1068.
- [32] Guorui Zhou, Xiaoqiang Zhu, Chenru Song, Ying Fan, Han Zhu, Xiao Ma, Yanghui Yan, Jin Junqi, Han Li, and Kun Gai. 2018. Deep Interest Network for Click-Through Rate Prediction. In *Proceedings of the 24th ACM SIGKDD International Conference on Knowledge Discovery & Data Mining (KDD)*. 1059–1068.
- [33] Chenxu Zhu, Bo Chen, Hufeng Guo, Hang Xu, Xiangyang Li, Xiangyu Zhao, Weinan Zhang, Yong Yu, and Ruiming Tang. 2023. AutoGen: An Automated Dynamic Model Generation Framework for Recommender System. In *Proceedings of the 16th ACM International Conference on Web Search and Data Mining (WSDM)*. 598–606.
- [34] Jie Zhu et al. 2025. RankMixer: Scaling Up Ranking Models in Industrial Recommenders. In *Proceedings of the 34th ACM International Conference on Information and Knowledge Management (CIKM)*. 6309–6316.